Intermodulation Product Computing Techniques for Broadband Active Transmit Systems

1 Learning Objectives

- From downloadable laboratory data, students will learn about compressive amplifiers for use in wideband systems.
- Students will learn about intermodulation products, harmonics, and fundamentals.
- Students will learn how to model an amplifier based on collected laboratory data.
- Students will learn about the discrete Fourier transform and its fast Fourier transform (FFT) implementation.
- Parseval's Theorem will be explored to determine the power of a signal in the time and frequency domains.

2 Introduction

The determination of intermodulation products is an ever pervasive problem to the radar and satellite community – its eminence will continue to manifest itself as data rates increase, as transmitters are required to handle increasing numbers of multiple carriers, and as amplifiers are pushed to operate closer to their non-linear regions (to circumvent the need of adding the extra weight and cost of a more linear amplifier). To study the intermodulation effects, FFT-based techniques are often employed. By definition, $\Delta = F_s/N$ defines the frequency resolution for the discrete Fourier transform. It is typically desired to design Δ to be as small as possible, to allow for a very fine frequency resolution. Doing this requires that F_s be minimized and/or N be selected as large as possible.

As reported in the literature, the ability to determine the amplitude and location of intermodulation products is of prime importance. Non-linear amplifiers lead to the generation of unwanted signal components that are mathematically related to the frequencies of input signals. It takes at least two tones at unique frequencies to generate these unwanted frequency components, known as intermodulation products. A few moments are taken here to visit the classic two-tone test; that is, when the input signal is defined by $v(t) = \cos(\omega_1 t) + \cos(\omega_2 t)$. The first order products are known as the frequencies of the original signals. The second order products are known as the second harmonics $\omega_1 + \omega_1$ and $\omega_2 + \omega_2$, and the sum and difference terms, $\omega_1 + \omega_2$, $\omega_2 + \omega_1$, $\omega_1 - \omega_2$, $\omega_2 - \omega_1$. The DC-terms $\omega_1 - \omega_1$ and $\omega_2 - \omega_2$ from the second-order distortions should be included in the list. The third order products are numerous, but the most vexing ones are the ones that occur close to or within the specified bandwidth of the transmission channel, since they are extremely tedious to remove by filtering and these are: $2\omega_1 - \omega_2$ and $2\omega_2 - \omega_1$. Continuing in a similar fashion, higher order products do exist.

In a gem of a paper, Hemmi explored the intermodulation product calculation problem oriented around the classic non-linear amplifier studies of Ha [5], but only considered the effects of a third order system [1]. Moreover, the upper bound of this work considered only exploring two tones. In his paper [3], Real also applied third order models to study the occurrence of intermodulation frequencies which result from amplifier non-linearities, but with more emphasis on

two-dimensional arrays (in this work, only one element of this array is considered). In contrast to the two works described above in which analytic equations were derived to determine the intermodulation product locations, high-order polynomials and multiple tones are considered here – which don't lend themselves to the construction of analytic equations. Here the memoryless power amplifier's nonlinear response is modeled as

$$e(t) = \alpha_0 + \alpha_1 v(t) + \alpha_2 v^2(t) + \alpha_3 v^3(t) + \alpha_4 v^4(t) + \alpha_5 v^5(t) \quad . \tag{1}$$

Polynomial models match our spectral laboratory data well. For completeness, it should be mentioned that other models do exist – the envelope model based on AM-AM and AM-PM distortions is popular. As noted by Loyka [6], this modeling technique is only valid for narrowband signals and systems – in contrast to the wideband system discussed here. Moreover, studying the effects of the intermodulation products of these multi-carrier systems typically requires a formidable amount of simulation time – in some cases. In an effort to rectify this problem, [2] has developed a partial-sum-of-products technique that is based on the decomposition of the signal at the output of the nonlinear device into a sum of products.

Employing the FFT to sequences of digitized multi-carrier simulated signals are often employed in the analysis of intermodulation products, particularly in designs that commission polynomial based models. A delicate balance of N, the number of samples taken, and F_s, the sampling rate, must be carefully achieved. The fundamentals, harmonics, and intermodulation products are modeled as spectral lines. Using the definition of the Fourier transform, $G(\omega) = \int_{-\infty}^{+\infty} g(t) e^{-j\omega t}\, dt$, the following transform pair is recalled

$$\mathscr{F}\{\cos(\omega_o t)\} = \pi[\delta(\omega - \omega_o) + \delta(\omega + \omega_o)] \quad , \tag{2}$$

where $\delta(\cdot)$ is the standard unit-impulse function. For comparative purposes later, the definition of the Fourier transform is applied here to derive the discrete Fourier transform as $\tilde{G}[k] = \sum_{n=0}^{N-1} \tilde{g}[n] e^{-j(2\pi/N)nk}$ for a discrete time sequence, $\tilde{g}[n]$, of N samples. Later in this module, this transform is implemented via the FFT, and its output sequence will be scaled by a factor of $1/\hat{N}$, under the proviso $\hat{N} = N/2$. This scaling is implemented so that the amplitudes of the continuous-time Fourier transform and the discrete-time Fourier transform will match when Δ is properly set. Nevertheless, it is noted that a variety of intermodulation analysis techniques rely on various implementations of the Fourier transform. For instance, Fortes and Sampaio-Neto relied on the discrete Fourier transform to design their fast algorithm that performs a selective counting of the third-order intermodulation products generated when several carriers are transmitted through a common nonlinear device [7]. The harmonic balance technique, which is popular for the study of modern microwave electronic circuits, is another technique that relies on the discrete Fourier transform inside of an iterative algorithm that is used to calculate steady state spectra generated by non-linear circuits. The harmonic balance technique was initially proposed in its simplest form by Baily [8], and has been used extensively in a variety of capacities by many, including [9, 10, 11, 12]. Finally, in the section that follows, the FFT is employed on sequences of digitized multi-carrier simulated signals.

2.1 Practical Systems & Example Results

In this section, the concern is when a large number of constant-amplitude carriers are involved, *i.e.*

$$v(t) = \sum_{k=1}^{M} V \cos(2\pi f_k + \theta_k) \quad , \tag{3}$$

which is then input to the nonlinearity defined by equation (1). It is noted that θ_k is a typical random phase shift, and V has constant amplitude. It is assumed that the input and output impedance of the two-port amplifier is described as $Z_{in} = Z_{out} = 50\Omega$, and the corresponding average input/output power is expressed as $10\log_{10}(V_{rms}^2 \cdot \frac{1000}{50\Omega})$ dBm, respectively, as defined in [5]. In general, for one carrier, $V_{rms} = V/\sqrt{2}$ for an input described by equation (3), where V is the peak value. For multiple carriers, each with random phases, such a closed form solution is not applicable, but a scaled version of the expression above is an appropriate place to start for simulated calculations. From Parseval's theorem, $V_{rms,out}$ can be determined by summing all of $e(t)$'s spectral components (the fundamentals, intermodulation products, and harmonics that are being sought here). For continuous time systems, this formula is recognized as

$$\int_{-\infty}^{\infty} |x(t)|^2 dt \;=\; \int_{-\infty}^{\infty} |X(f)|^2 df \quad . \tag{4}$$

For discrete signals, it is expressed as

$$\sum_{i=0}^{N-1} |x[i]|^2 \;=\; \sum_{k=0}^{N-1} |X[k]|^2 \quad . \tag{5}$$

In the laboratory, the compressive amplifier system to be modeled in this study is described by two specifications: 1.) given a -16 dBm input, it has a 40 dBm output, yielding a 56 dB gain, and 2.) at a -6 dBm input level, it is expected to have a 50 dBm output, but this input level defines the system's 1 dB compression point, thus an output of 49 dBm is obtained. From these specifications, the output voltage of the amplifier under test can be modeled as a fifth order polynomial, described by equation (1), which has coefficients defined by $[\alpha_5,\ \alpha_4,\ \alpha_3,\ \alpha_2,\ \alpha_1,\ \alpha_0]$ = (1.0e+004)[-1.32572477906842, 1.49300774042668, -0.56771010070975, 0.00991337349828, 0.06379850352323, 0.00000246]. As the compressive amplifier is modeled by equation (1), spectral contributions are modified by α_q, for $q = 1, ..., d$, where d denotes the highest degree in the polynomial. In the Activities section of this module, a similar compressive amplifier will be studied, and its governing polynomial will be determined by laboratory data.

Here, a select group of frequencies within a specific band is considered. The carrier frequencies are in the band of 115 to 160 MHz. These carrier frequencies are $\boldsymbol{f}$ = [115, 121, 124, 132, 135, 140, 151, 160] MHz, which define the multi-tone input signal. Figure 1 depicts the spectral content of the amplifier's output with the FFT. Owing to the large dynamic range, the vertical axis on these plots employs the log scale, *i.e.* $10\log_{10}\{\cdot\}$ dB. In this analysis, $N = 524288$ and $F_s = 2 \cdot 5 \cdot 160$ MHz = 1600 MHz.

Often times, it is desired to make a plot of the intermodulation products and fundamentals in a particular band of interest. This band is a region near and inclusive of the fundamental or carrier frequency components of the spectrum. In a typical system, in which there is an abundance of fundamental components, the goal is to determine the height of the intermodulation products relative to the carrier frequency components, i.e. dBc. Figure 2 depicts the 100 to 190 MHz band, which encompasses the previously mentioned frequency band of interest. The eight tones appear at their respective frequencies, while the other spectral lines are intermodulation products. The harmonics are not shown in this figure, since they occur at integer multiples of the fundamental frequencies. Within the plot, the fundamental components have been rescaled to 0 dB. Here, the height of the intermodulation products relative to the carrier frequency components is 12 dBc, based on the most intrusive intermodulation product located at 155 MHz.

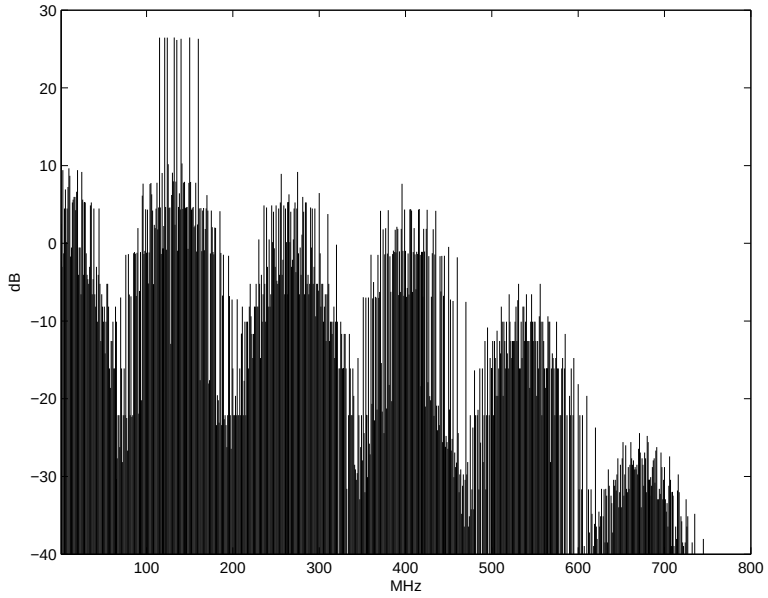

Figure 1: *Analysis via the FFT, which depicts the intermodulation products, fundamentals, and harmonics.*

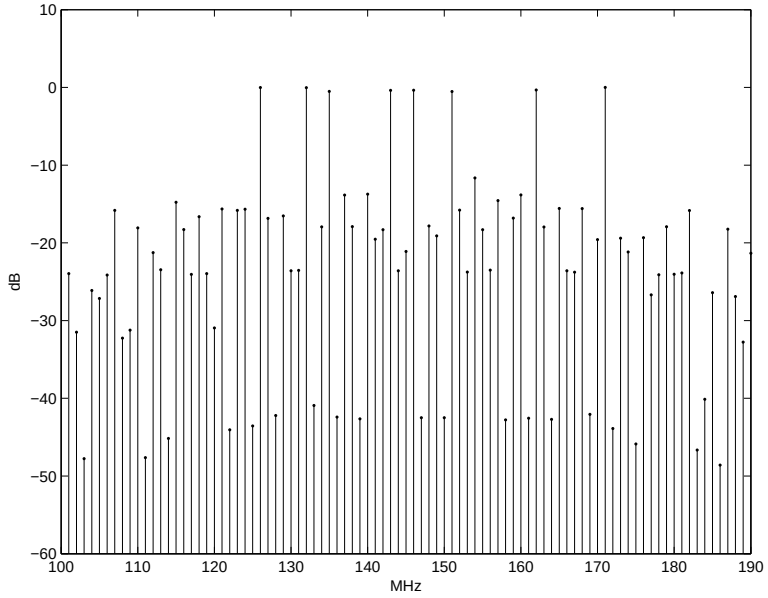

Figure 2: *Location of the intermodulation products and fundamentals within the vicinity of the frequency band of interest. Scaling has been implemented so that 0 dB corresponds to the maximum amplitude of the fundamental components.*

2.2 Importance of Intermodulation Terms

Intermodulation terms have an influence on the performance of a variety of RF systems. For instance, in a system that relies on beamforming and multicarrier UHF power amplifiers, the non-linear effects of the amplifiers will also be propagated with each specific beam. For the example in Figure 3, each beam is split up and multiplied by a unique set of beamforming coefficients and carefully routed to an amplifier for subsequent transmission. Within each beam, intermodulation terms are present. This simulation also includes system noise and digital quantization effects (8 bit words).

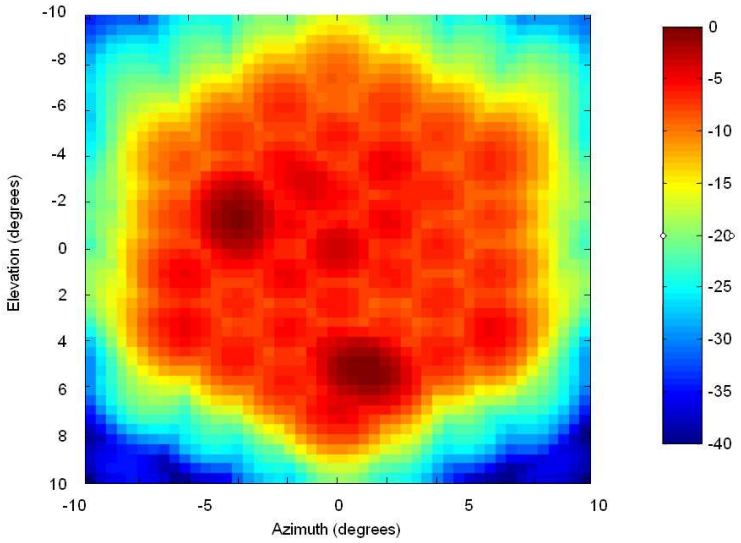

Figure 3: *Beam pattern of two transmitted beams which also include the system's non-ideal effects.*

3 Hands-On Activities

1. To model the effects of a real compressive amplifier driving an array based system, the amplifier can be modeled as a polynomial. In the past, this polynomial has taken the form $e(t) = a_1 v(t) + a_2 v^2(t) + a_3 v^3(t)$. For the input $v(t) = \cos(\omega_1 t) + \cos(\omega_2 t)$, it is mathematically feasible to derive closed-form mathematical expressions for the system in the pursuit of intermodulation products. *For a general case of a_1, a_2, a_3, ω_1, and ω_2, provide an expression for $e(t)$ and by using a table carefully explain the location of the intermods, harmonics, and fundamentals.* Read the paper by Hemmi [1] to assist your discussion.

2. For item 1, what happens when a_2 and a_3 become very small relative to a_1, say $a_2 << a_1$ and $a_3 << a_1$.

3. When $v(t)$ is comprised of a large number of carrier frequencies and when the order of the polynomial grows, the system becomes extremely tedious to track with closed-form mathematical expressions. *Explain how FFT based solutions are typically employed to analyze an amplifier's output.*

4. Using the laboratory data, provide a plot of the output power in dBm vs. the input power in dBm. Here, voltage data are given, and it is assumed that 50 Ω terminations were used.

   - www.ou.edu/radar/VinVoutAmplifier.m
   - Your plot should appear similar to Figure 4. Be careful to note the units on the axis. These input voltages correspond to power that was applied to the amplifier at a constant frequency to characterize the amplifier in terms of its power characteristic.
   - Pick a point in the linear region, and the power gain should be approximately 56 dB. As a conservative estimate, this region is anywhere below an input power of -10 dBm.

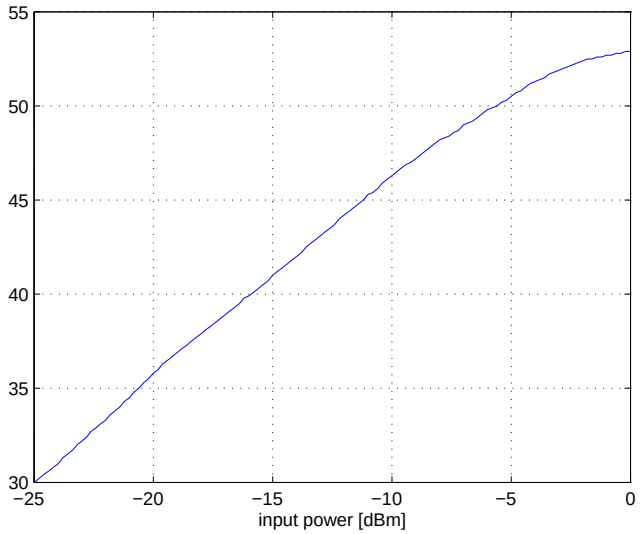

Figure 4: *Plot of the input and output power as determined from the laboratory data.*

5. Using Matlab's "polyfit" command, determine a polynomial fit for the data to model the amplifier. Choosing the model's order is your choice (for this data, a fifth order has worked well in the past). Be sure to use the *format long* command in Matlab to see many significant digits in the coefficients. For this particular data, you should see these coefficients 1.0e+004*[-3.383130356644798, 3.462033869678062, -1.464696216469087, 0.175515947868355, 0.059636354161487, -0.000108994958695]. Here, the first coefficient corresponds to α_5.

6. From the previous step, use the *polyval* command to evaluate the input voltage data with the new model. Make a plot of Vout vs. Vin with the lab data (note: this is voltage data, not power data). Then, on the same graph, make a plot of Vout,new vs. Vin using the model. Do both voltage curves appear similar? You should also try a 3rd order model and plot it on the same graph as well. Be sure to use different colors, symbols, dashed lines, etc. – labeling or legends are preferred.

7. Set up an experiment to model a set of frequencies, similar to the Introduction Section: [115, 121, 124, 132, 135, 140, 151, 160] MHz, which define the multi-tone input signal. Let the average input power of the signal be between -20 dBm and -15 dBm. This will ensure that the amplifier is being operated in its linear region.

    - This signal is to be a digital signal that is to be processed later by the FFT. By definition, a digital signal $v(k) = v(t)|_{kT_s}$. For the FFT, the resolution is defined as $\Delta = F_s/N$. As such, F_s needs to set reasonably large to avoid aliasing, and N should be as large as possible. Given that the highest frequency to be sampled is 5×160 MHz, here a value of F_s can be established as 1600 MHz or more. Note: for the simulations, MHz may be scaled to Hz for convenience.
    - Each carrier within the model also needs to have a uniformly distributed random phase, in the range of $-\pi$ to π.
    - A representative expression of the input signal appears as follows: (v)*(sin(f1*d +p1) + sin(f2*d +p2) + ... + sin(f8*d +p8), where d=2*pi*i*Ts for i=0 to N.
    - To avoid smearing in the digital spectrum, it is recommended that each frequency, f1 to f8, be assigned a unique spectral line. That is, each frequency should not occupy multiple frequency bins in the FFT. To ensure this, each analog frequency should be re-expressed as an integer multiple of F_s/N. For instance, 115 Hz is represented as f1 = 37683*(Fs/N) = 114.99938964843 Hz. The student should decide the appropriate integer multiple.
    - Determine the signal's power. Let the sum be comprised of the addition of (v(i)/ sqrt(2))^2 for each i. Using vectors, let signalsum = v^{T}v /2. Let inrms = sqrt(signalsum/N) and meanpower = 10*log10(inrms*inrms*1000/50).

8. Make a simulation to find the average output power, and confirm it withe the plot above. As an example calculation, results reveal that if an input power of -17.2809 dBm is impressed upon the system, then an output power of 38.7199 dBm may be calculated. This yields a difference of 56.0008 dB, which is expected.

9. Use the FFT to prepare a plot of the output's spectrum. Discuss your approach to predict precisely the position and magnitude of the spectral components of a multi-tone signal where all carriers have equal magnitude and phase. The plot should resemble 5.

    - Your magnitude plot should encompass 100 dB of dynamic range on the verticle axis. The frequency axis should span DC to $F_s/2$.
    - Make another plot by carefully zooming into region near the fundamental components. Determine the dBc.

- Using Parseval's theorem, calculate the power of the output signal in the time domain and calculate the power of the signal in the frequency domain. Show that they are equivalent.

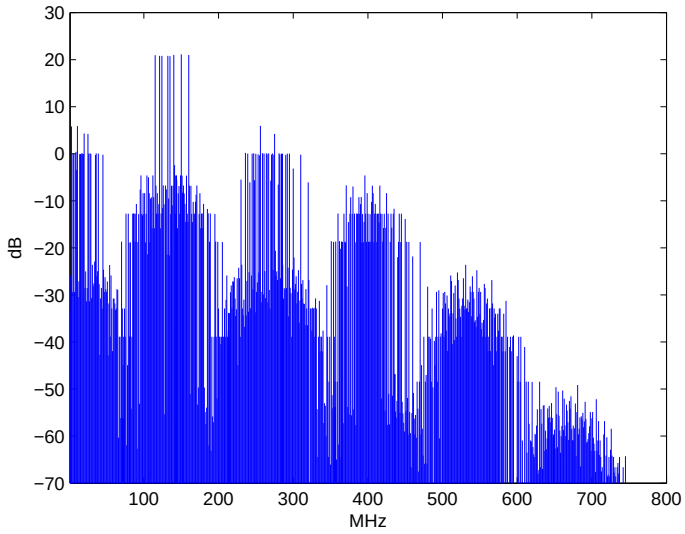

Figure 5: *FFT of the Output. The fundamental components, intermodulation terms, and harmonics are depicted for the compressive amplifier.*

10. Increase the input power to approximately -3 dBm. Discuss how the strength of the intermodulation products has been increased. Repeat the Step 9 and discuss all of the details.

11. Bonus: the especially interested student is encouraged to read the book by Ha [5] and other books for more understanding about this topic.

References

[1] C. Hemmi, "Pattern characteristics of harmonic and intermodulation products in broad-band active transmit arrays," *IEEE Trans. on Antennas and Prop.*, vol. 50, no. 6, June 2002.

[2] K. Schneider and W. Tranter, "Efficient simulation of multicarrier digital communication systems in nonlinear channel environments," *IEEE J. on Selected Areas in Comm.*, vol 2, no. 3, April, 1993.

[3] E. Real and D. Charette, "Non-linear amplifier effects in transmit beamforming arrays," *IEEE International Conference on Acoustics, Speech, and Signal Processing*, vol. 5, pp. 3635-3638, 1995.

[4] W. Sandrin, "Spatial distribution of intermodulation products in active phased arrays," *IEEE Trans. Antennas and Prop.*, vol. 21, pp. 864-868, Nov. 1973.

[5] T. Ha, *Solid State Microwave Amplifier Design*, New York: Wiley, 1981.

[6] S. Loyka, "The influence of electromagnetic environment on operation of active array antennas: analysis and simulation techniques," *IEEE Antennas and Propagation Magazine*, vol. 41, no. 6, pp. 23-39. Dec. 1999.

[7] J. Fortes and R. Sampaio-Neto, "A fast algorithm for sorting and counting third-order intermodulation products," *IEEE Transactions on Communications*, vol. 34, no. 12, pp. 1266-1272, December 1986.

[8] E. Baily, "Steady state harmonic analysis of nonlinear networks," *Ph.D. Thesis*, Stanford University. http://library.stanford.edu, Stanford, CA, 1968.

[9] M. Nakhla and J. Vlack, "A piecewise harmonic balance technique for determination of periodic response of nonlinear systems," *IEEE Transactions on Circuits and Systems*, vol. CAS-23, February 1976.

[10] V. Borich, J. East, and G. Haddad, "An efficient Fourier transform algorithm for multitone harmonic balance," vol. 47, no. 2, pp. 182-188, February 1999.

[11] F. Rotella, G. Ma, Z. Yu, and R. Dutton, "Modeling, analysis, and design of RF LDMOS devices using harmonic balance device simulation, *IEEE Transactions on Microwave Theory and Techniques*, 48(6):991-999, 2002.

[12] V. Rizzoli, A. Neri, F. Mastri, and A. Lipparini, "Modulation-oriented harmonic balance based on Krylov-subspace methods," *IEEE MTT-S International Microwave Symposium*, pp. 771-774, June 1999.

[13] T. Närhi, "Black-box modeling of nonlinear devices for frequency domain analysis," *Proc. 21st European Microwave Conference,* pp. 1109-1114, August 1992.

[14] T. Närhi, "Frequency-domain analysis of strongly nonlinear circuits using a consistent large-signal model," *IEEE Transactions on Microwave Theory and Techniques,* vol. 44, no. 2, pp. 182-192, February 1996.

[15] C. Chang and M. Steer, "Frequency-domain nonlinear microwave circuit simulation using the arithmetic operator method," *IEEE Transactions on Microwave Theory and Techniques,* vol. 38, no. 8, pp. 1139-1143, August 1990.

[16] N. de Carvalho and J. Pedro, "Multitone frequency-domain simulation of nonlinear circuits in large-and small-signal regimes," *IEEE Transactions on Microwave Theory and Techniques,* vol. 46, no. 12, part 1, pp. 2016-2024, December 1998.

[17] G. Rhyne and M. Steer, "Frequency-domain nonlinear circuit analysis using a frequency-domain harmonic balance technique," *IEEE Transactions on Microwave Theory and Techniques,* vol. 36, pp. 379-387, February 1988.